

Feedforward and Feedback Control Behavior in Helicopter Pilots during a Lateral Reposition Task

F. M. Drop^a, D. M. Pool^b, M. M. van Paassen^b, M. Mulder^b, H. H. Bühlhoff^{a,c}

^a{frank.drop, heinrich.buelthoff}@tuebingen.mpg.de

^b{d.m.pool, m.m.vanpaassen, m.mulder}@tudelft.nl

^aMPI for Biological Cybernetics, Tübingen, Germany

^bDelft University of Technology, Delft, the Netherlands

^cKorea University, Seoul, Korea

ABSTRACT

Pure feedback and pure open-loop feedforward helicopter pilot models are currently applied for predicting the performance of pilot-helicopter systems. We argue that feedback models are likely to underestimate performance in many realistic helicopter maneuvers, whereas inverse simulation models, which have an open-loop feedforward structure, are likely to overestimate performance as they neglect typical human-in-the-loop characteristics. True verification of feedback and feedforward elements in helicopter pilot control behavior was never performed, however. This paper proposes a pilot model containing a feedback and feedforward controller acting simultaneously and presents a method to identify the hypothesized feedforward action from human-in-the-loop data collected in a simulator experiment. The results of the human-in-the-loop experiment show that actual human performance is better than predicted by a pure feedback model and worse than predicted by an (inverse dynamics) feedforward model. The identification results suggest that the human pilot indeed utilizes feedforward strategies, but it was not possible to either confirm or refute the model by means of the collected data and the developed analysis method.

INTRODUCTION

A mathematical model of helicopter pilots' manual control behavior is useful for offline simulations to evaluate and quantify pilot-helicopter system performance early in the design stage. Different types of pilot models are used for different applications, such as shipboard operations (Refs. 1, 2) and ADS-33 certification maneuvers (Refs. 3, 4).

The pilot models described for such applications in literature differ mainly in whether they have a feedback or an open-loop feedforward structure. In this paper, we define a feedback controller as a controller that operates on the error between the commanded flight path and the current output of the helicopter. An open-loop feedforward controller is defined as a controller that takes the commanded flight path as the sole input and generates the appropriate control signal to steer the helicopter along this reference trajectory.

In control systems, feedback is necessary for stability and will provide a basic level of performance. The performance can be improved by adding a feedforward path, where the optimal feedforward controller is equal to the inverse of the system dynamics. We hypothesize that the human pilot makes use of similar feedforward control strategies for certain helicopter maneuvering tasks to significantly improve his perfor-

mance. This paper will investigate this hypothesis by developing a method to objectively *identify* human control behavior from actual human-in-the-loop measurements. Additionally, this paper will investigate the consequences of including a feedforward path in a pilot model for offline simulations used to quantify pilot-helicopter system performance.

Feedback pilot models are usually based on the Crossover model of McRuer *et. al* (Refs. 5, 6), the Structural Model of Hess (Refs. 1, 7) or the Optimal Control Model of Kleinman *et. al* (Refs. 2, 8). Such models are usually straightforward to implement and are based on objective measurements of human control behavior. It is, however, important to note that these feedback models were intended to describe pilot dynamics in tracking tasks with quasi-random target or disturbance signals that appear unpredictable to the human (Refs. 6–8). In real helicopter flight, however, the pilot is not tracking an erratic reference path, but performs goal-directed maneuvers such as forward flight, turns and climbs, hover pedal turns, bob-up maneuvers and longitudinal and lateral repositions. The feedback models do not take the cognitive capabilities of the human that play an important role during such maneuvers into account, such as his ability to acquire an internal model of the system dynamics through learning, to make predictions on the future course of the target and to use memorized knowledge. One might therefore expect that purely feedback models *underestimate* the performance of the pilot-helicopter system for realistic maneuvers.

Presented at the AHS 69th Annual Forum, Phoenix, Arizona, May 21–23, 2013. Copyright © 2013 by the American Helicopter Society International, Inc. All rights reserved.

The open-loop feedforward pilot models that are sometimes used in helicopter applications are usually described in *inverse simulation* problems (Refs. 3, 4, 9–11). In inverse simulations, a desired flight trajectory and the ‘forward’ helicopter equations of motion are given, from which the corresponding control signal is calculated, usually done by numerically inverting the helicopter dynamics. Although the inverse solution might resemble the complex cognitive abilities of the human pilot better than a pure feedback model, it does not, in its most basic form, explicitly consider any human-in-the-loop effects. As such, it might not be representative for what the pilot-helicopter system can do, because 1) the pilot does not know or cannot execute the optimal control signal, 2) the pilot needs to leave margin to structural load limits, 3) the pilot will also have to cope with unpredictable external disturbances, and 4) because the pilot is unwilling or is trained not to perform extreme maneuvers in certain flight conditions, e.g. close to the ground (Ref. 9). Therefore, inverse simulation models are likely to *overestimate* the performance of the pilot-helicopter system for realistic maneuvers.

Several authors have addressed the problem of overestimation by the inverse simulation approach and proposed alternative model structures that model intrinsic limitations of the pilot (Refs. 4, 10, 11) and performed human-in-the-loop experiments to compare the inverse simulation result to human data (Ref. 9). Still, none of the previous works have considered the possibility that the human pilot might operate a feedback loop and a feedforward path *simultaneously* and neither did they attempt to objectively measure pilot control behavior, for example through system identification techniques, to validate their proposed model. As such, a pilot model for realistic helicopter tasks, taking into account both feedback and feedforward control behavior, based on human-in-the-loop measurements does not exist.

It is the objective of this paper to develop a helicopter pilot model that takes both feedback and feedforward control behavior into account and to 1) show the difference in performance between a pilot model with and without an inverse system dynamics feedforward path and 2) to identify from experimental data whether or not the human pilot employs such feedforward control techniques. We hypothesize that 1) the difference in performance between the two approaches is large in a realistic control task and that 2) evidence of feedforward behavior can be identified from experimental data.

System identification methods that can be used to identify human control behavior require the control task to be a tracking task, where the human pilot is required to accurately follow an explicitly presented target object or marker. Within the wide range of realistic helicopter maneuvers, only few will require such accurate control. We argue, however, that ADS-33 certification tasks generally require highly accurate control, such that they can be represented as tracking tasks and induce very similar control behavior in the human pilots. Therefore, this paper will study the hypotheses by means of a tracking task resembling an ADS-33 lateral reposition maneuver (Ref. 12).

The paper is structured as follows. First, we introduce the ADS-33 lateral reposition maneuver and investigate from a control theoretical perspective what control dynamics can be expected to play a role in this control task. Then, we perform simulations to investigate the performance effect of a feedforward element, after which we investigate to what extent it is possible to identify from measured data whether the human pilot is using feedforward strategies. After describing the human-in-the-loop experiment and its results, the paper will end with a discussion and conclusions.

ADS-33 LATERAL REPOSITION TASK

This paper studies pilot control dynamics in a tracking task that resembles the ADS-33 lateral reposition task. This task is intended to check the roll and heave axis handling qualities during moderately aggressive maneuvering. The task consists of accelerating laterally from a stabilized hover at 35 ft wheel height up to a lateral ground speed of approximately 35 knots followed by a deceleration to laterally reposition the rotorcraft in a stabilized hover 400 ft down the course (Ref. 12).

A reference trajectory (or: *target signal*) was constructed which meets the Good Visual Conditions (GVE) desired performance requirements for cargo/utility rotorcraft, i.e. to complete the maneuver within 18 seconds, see Fig. 1. Directly af-

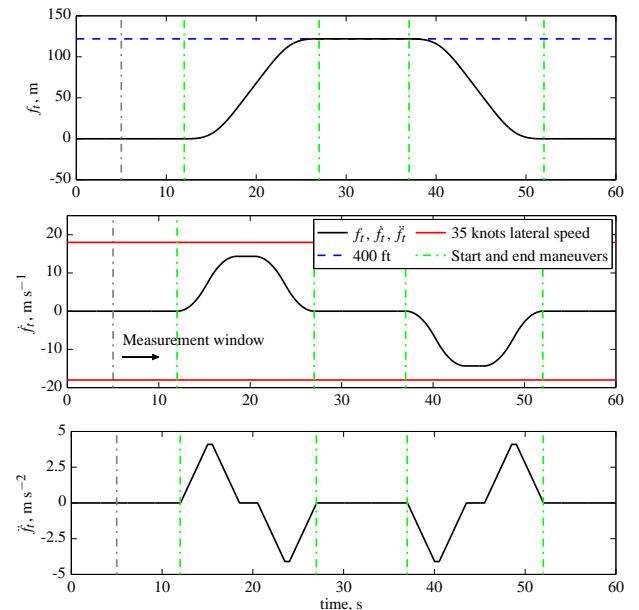


Fig. 1. The lateral target signal f_l and its time derivatives.

ter performing one lateral reposition to the right (positive \dot{f}_l is motion to the right) an identical reposition to the left is to be made. The green lines mark the start and end of the two lateral repositions which by themselves take exactly 15 seconds. This is 3 seconds shorter than the requirement of 18 seconds to account for the time the pilot needs to acquire a stable hover. The target signal presented in Fig. 1 is used throughout all simulations in this paper, as well as in the human-in-the-loop experiment.

We will only consider the roll and lateral dynamics of the helicopter, such that the other performance requirements relating to longitudinal, vertical and heading motion do not play a role in our analysis.

MODEL OF PILOT CONTROL DYNAMICS

In this section we study the task of the pilot during the ADS-33 lateral reposition from a control theoretical perspective, but constrain the model to the physiological abilities of the human pilot. That is, the model will not make use of signals that can not be perceived by the human senses and will contain a model of the neuromuscular system. The primary senses of the pilot are vision and the vestibular system; the contribution of both will be discussed next.

A schematic representation of the out-of-the-window visuals during the task is given in Fig. 2, which shows that four ‘fundamental’ signals can be perceived directly from the display: the lateral target signal f_t , the helicopter roll angle ϕ , the helicopter lateral position y and the lateral tracking error $e_y = f_t - y$. We assume that all linear and rotational veloci-

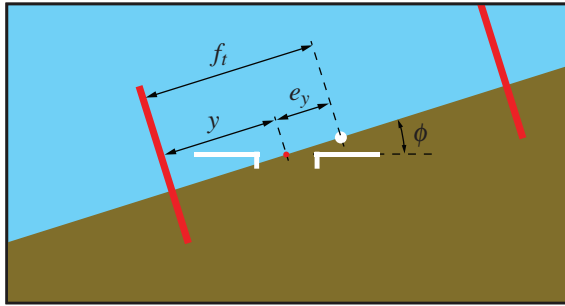


Fig. 2. A schematic representation of the out-of-the-window visuals. The white aircraft symbol marks the current lateral position and roll angle of the helicopter. The white dot indicates the tracking target. Lateral tracking error e_y is to be minimized by the pilot. Recognizable objects, such as the red poles, act as fixed reference points for the target and helicopter lateral position.

ties (\dot{f}_t , \dot{e}_y , \dot{y} and $\dot{\phi}$) can also be perceived by means of the visual system, but that accelerations can not be perceived visually (Ref. 13). Visual perception is usually associated with considerable time delays, typically 0.1 to 0.3 seconds (Ref. 6).

We assume the vestibular system to be able to perceive linear accelerations (\ddot{y}) and rotational velocities, $\dot{\phi}$ (Ref. 14). Typical time delays associated with the vestibular system, measured in closed loop control tasks, are 0.2 seconds (Ref. 15).

Finally, an important feature of the target signal is that it is identical throughout the entire experiment which enables the human pilot to learn and memorize its relevant features and use these for more effective control (Ref. 16).

Control scheme

A schematic block diagram of the lateral reposition task and the proposed pilot control model is given in Fig. 3. The blocks

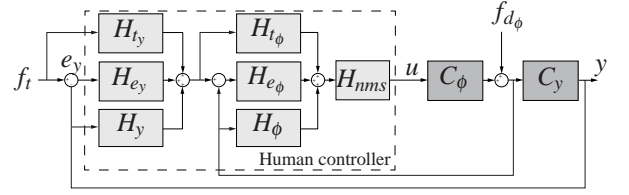


Fig. 3. Schematic representation of the lateral reposition task and the proposed pilot model.

contained within the dashed box are internal to the pilot, the blocks $C_\phi(s)$ and $C_y(s)$ represent the roll and lateral dynamics of the helicopter, respectively. For the simplified helicopter model considered in this paper, these dynamics are given as:

$$C_\phi(s) = \frac{K_{c_\phi}}{s}, \text{ with } K_{c_\phi} = 1.2 \quad (1)$$

$$C_y(s) = \frac{K_{c_y}}{s^2}, \text{ with } K_{c_y} = 9.81 \quad (2)$$

Signal f_{d_ϕ} is a disturbance signal and models the presence of turbulence.

We assume a serial model structure (rather than a parallel model structure) in which the pilot first closes and stabilizes the inner (roll) loop and then the outer (lateral position) loop. For both the roll and the lateral loop we consider three pilot control elements: one feedforward path, one error feedback element and one feedback element responding to the respective output signal of the helicopter. Both the inner and the outer loop have an individual feedforward element, as opposed to one feedforward element taking f_t as input and giving an output directly to u . This is necessary to prevent the roll loop feedback element $H_{e_\phi}(s)$ to ‘fight’ (and thereby cancel) the inputs of such a feedforward element.

Roll loop feedback The roll loop contains the helicopter roll dynamics and all the inner loop pilot control elements, see Fig. 4. The roll target signal ϕ_t is not a measurable signal because it is internal to the pilot and thus e_ϕ is also not measurable. Therefore, the feedforward element $H_{t_\phi}(s)$ and the error feedback element $H_{e_\phi}(s)$ respond to internal signals. The state feedback element $H_\phi(s)$ is the only element responding to a signal that is directly measurable and perceivable.

The dynamics of the neuromuscular system and the control manipulator are described by $H_{nms}(s)$ and are commonly modeled as a second-order system,

$$H_{nms}(s) = \frac{\omega_{nms}^2}{s^2 + 2\zeta_{nms}\omega_{nms}s + \omega_{nms}^2} \quad (3)$$

with natural frequency $\omega_{nms} = 12$ rad/s and damping ratio $\zeta_{nms} = 0.2$ (Ref. 17).

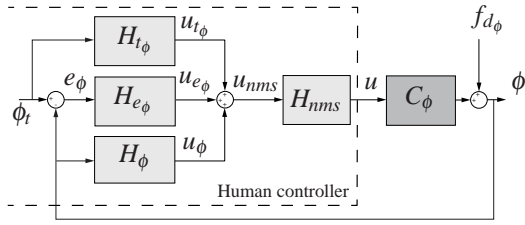


Fig. 4. Schematic representation of the inner (roll) loop, containing pilot feedback and feedforward elements, helicopter roll dynamics and roll disturbance signal f_{d_ϕ} . The roll target signal ϕ_t only exists in the pilot and is generated by the outer loop controller.

The stability and disturbance-rejection properties of the roll loop are determined by H_{e_ϕ} and H_ϕ . The dynamics of H_{e_ϕ} necessary to achieve stability will depend on the content of H_ϕ and vice versa. In general, the primary use of ‘state feedback’ elements, such as H_ϕ , are to stabilize the system dynamics and to improve the disturbance rejection performance of the controller.

For the single integrator roll dynamics one can derive that choosing a gain for H_ϕ will improve the disturbance rejection performance of the controller, but will simultaneously *worsen* the target-tracking performance. The decrease in target-tracking performance is especially large due to the considerable time delay that is present in the state feedback generated by the human pilot (Ref. 15). In this task the overall task performance is primarily determined by the controller’s target-tracking performance, because disturbances will be relatively small compared to the size of the maneuver itself. Therefore, we assume the contribution of the state feedback to be negligibly small and thus assume $H_\phi(s)$ to be equal to zero.

For single integrator dynamics we can model the error feedback path H_{e_ϕ} as a gain and a time delay, based on the Crossover Model (Ref. 6).

$$H_{e_\phi}(s) = K_{e_\phi} e^{-\tau_{e_\phi} s} \quad (4)$$

A typical value of K_{e_ϕ} is 2.5, such that the crossover frequency of the inner loop is equal to 3.0 rad/s. A typical value for the time delay τ_{e_ϕ} for single integrator dynamics is 0.25 seconds (Ref. 18).

Roll loop feedforward If we assume the internal signal ϕ_t to be known to the pilot and of predictable nature, we expect the pilot to perform a feedforward operation on ϕ_t , based on the results of Ref. 18. Ref. 18 investigated feedforward control strategies in a single-loop pitch-axis tracking task with predictable target signals and found that feedforward control behavior similar to inverse system dynamics can readily be identified from experimental data. As can be verified from Fig. 3, the ideal feedforward dynamics H_{I_ϕ} are equal to the inverse system dynamics: (Ref. 19)

$$H_{I_{\phi_{\text{ideal}}}}(s) = \frac{u(s)}{\phi_t(s)} = \frac{1}{C_\phi(s)} \Rightarrow u(s) = \frac{1}{C_\phi(s)} \phi_t(s). \quad (5)$$

The system output ϕ is then found to be:

$$\phi(s) = C_\phi(s) \cdot u(s) = C_\phi(s) \cdot \frac{1}{C_\phi(s)} \cdot \phi_t(s) = \phi_t(s). \quad (6)$$

That is, output ϕ is exactly equal to the target signal ϕ_t , yielding zero tracking error. We thus assume the inverse of the helicopter roll dynamics for H_{I_ϕ} , see Eq. 7.

$$H_{I_\phi}(s) = K_{I_\phi} \frac{1}{C_\phi(s)} = K_{I_\phi} \frac{s}{1.2} \quad (7)$$

Gain K_{I_ϕ} is added to be able to tune the amount of feedforward action. For optimal performance $K_{I_\phi} = 1$; for no feedforward contribution $K_{I_\phi} = 0$.

Lateral loop feedback The outer loop commands roll angles (ϕ_t) to the inner loop and thereby controls the lateral dynamics of the helicopter, see Fig. 5. In Fig. 5, the inner-loop pilot dy-

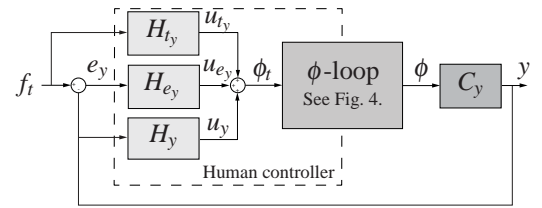


Fig. 5. The lateral loop isolated from the complete loop.

namics and helicopter dynamics are represented simply by the block ‘ ϕ -loop’. If we assume the roll loop to be well-tuned, we can approximate it as a gain close to unity and thereby simplify the analysis of the lateral loop below. The stability of the controller is determined by H_y and H_{e_y} and their dynamics mutually depend on each other.

One can derive that rate feedback is the most effective form of state-feedback for the outer loop, i.e. $H_y(s) = K_y s e^{-\tau_y s}$. However, as also discussed for the roll loop, the state feedback only improves the disturbance-rejection performance of the pilot-helicopter system, but worsens the target-tracking performance. Since this task primarily relies on target-tracking performance, we expect that the contribution of the state-feedback is only small and therefore we will neglect it in the remainder of the paper. Hence, we assume $H_y(s) = 0$.

Based on the Crossover Model of McRuer *et. al* (Ref. 6) we expect the error feedback element H_{e_y} to be a gain at low frequencies and a lead at higher frequencies:

$$H_{e_y}(s) = K_{e_y} (T_{e_y} s + 1) e^{-\tau_{e_y} s} \quad (8)$$

Typically, the outer loop crossover frequency is approximately one third of the inner loop crossover frequency (Ref. 1), but since we are considering an aggressive maneuver we will choose model parameters that lead to slightly better performance. That is, we choose $K_{e_y} = 0.15$ and $T_{e_y} = 1$ seconds such that the outer loop crossover frequency is approximately 1.5 rad/s. Furthermore, we set the outer loop time delay τ_{e_y} to 0.1 seconds, such that the total feedback time delay (including the roll feedback delay of 0.25 s) becomes 0.35 seconds.

Lateral loop feedforward Similar to the roll loop, we hypothesize that the pilot performs a feedforward operation to improve the tracking performance. For optimal performance the feedforward element H_{t_y} should be equal to the inverse of the lateral dynamics:

$$H_{t_y} = K_{t_y} \frac{1}{C_y(s)} = K_{t_y} \frac{s^2}{9.81} \quad (9)$$

The gain K_{t_y} was added such that the contribution of the feedforward path can be tuned.

Model development conclusions

In the previous section a pilot model was developed for a roll-lateral helicopter control task, assuming the helicopter dynamics as defined in Eqs. 1 and 2. The model was developed from a control theoretical perspective, but the possible model elements were constrained to respond to signals that are perceivable by the human pilot. The important conclusions and findings are 1) that concerning the roll-loop feedback elements the likely form of H_{e_ϕ} is a gain and a time delay, 2) that concerning the lateral-loop feedback elements the likely form of H_{e_y} is a gain at low frequencies and a lead at higher frequencies, 3) that these two findings result in identical controller dynamics for H_{e_ϕ} and H_{e_y} , as were proposed by McRuer *et. al* for steady-state compensatory tracking (Ref. 6).

Furthermore, the objective of this paper can now be formulated more precisely by means of Fig. 3, i.e., it is our objective to 1) investigate the difference in performance between a model containing H_{t_y} and H_{t_ϕ} , and a model without these elements, and 2) to identify from experimental data whether or not the human pilot indeed performs feedforward control behavior similar to inverse system dynamics for H_{t_y} and H_{t_ϕ} .

PERFORMANCE SIMULATIONS

This section addresses the first objective of this paper, that is, to investigate the difference in performance between purely feedback behavior and a combination of feedback and feedforward behavior. Simulations are performed using the model developed in the previous section and performance is measured by the maximum value of the lateral tracking error e_y occurring at any time during the simulation.

The performance of a controller depends on its target-tracking performance and its disturbance-rejection performance, which are two separate qualities. For a purely feedback controller a trade-off between the two qualities has to be found. However, a controller containing feedforward can use its feedforward path for target tracking and use the feedback loop to cope with the disturbances. As such, the usefulness of a feedforward element will depend on the presence, and strength, of disturbances such as turbulence. For small to moderate disturbances, the feedforward element will have a considerable contribution to the tracking performance. However, for large disturbances, the overall performance of the controller is largely determined by its disturbance-rejection

performance and thus the contribution of the feedforward element is only small.

Because the usefulness of the feedforward element is dependent on the strength of the disturbance signal, the simulations were performed as a function of the standard deviation of disturbance signal f_{d_ϕ} , which disturbs the roll angle directly, see Fig. 3, and is identical to the disturbance signal described in the Experiment section. The pilot model parameter values as used during the simulations are given in Table 1. Four different settings of the pilot model are defined, being a pure feedback model (FB), a model containing feedback and roll feedforward (RFF), a model containing feedback and lateral feedforward (LFF) and a model containing feedback and both roll and lateral feedforward (RLFF).

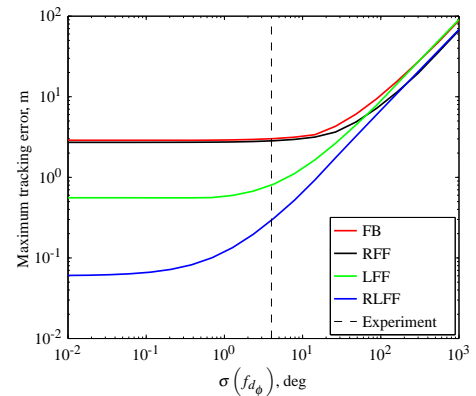


Fig. 6. Tracking performance as a function of the roll disturbance signal magnitude.

Fig. 6 shows the maximum tracking error for four different settings of the pilot model as a function of the standard deviation of the disturbance signal f_{d_ϕ} . Note that the maximum lateral error is plotted on a logarithmic scale. The differences are, as expected, largest for small to moderate disturbances. Roll feedforward by itself (RFF model) improves the performance only marginally compared to the purely feedback case (FB model), but the sole addition of lateral feedforward (LFF model) greatly improves performance. Obviously, the best performance for small to moderate disturbances is obtained by the model containing both roll and lateral feedforward (RLFF model). For larger disturbances the differences are very small, but feedforward still improves the performance (especially roll feedforward).

For a disturbance signal with a standard deviation of 4 deg, which falls within the range of what can be argued to be realistic disturbance magnitudes, the maximum lateral tracking error of the FB model is in the order of 3 m. The RLFF model, containing both roll and lateral feedforward, has a maximum error of only 0.26 m, which is one order of magnitude smaller. This shows the importance of a proper pilot model, if it were to be used for a simulation early in the design phase to determine the roll lateral performance of the helicopter in an absolute sense.

Table 1. Four model parameters sets used in simulations throughout this paper.

Element	Feedback, FB	Roll Feedforward, RFF	Lateral Feedforward, LFF	Full Feedforward, RLFF
$H_{t_y}(s) = K_{t_y} \frac{s^2}{9.81}$	$K_{t_y} = 0$	$K_{t_y} = 0$	$K_{t_y} = 1$	$K_{t_y} = 1$
$H_{t_\phi}(s) = K_{t_\phi} \frac{s}{1.2}$	$K_{t_\phi} = 0$	$K_{t_\phi} = 1$	$K_{t_\phi} = 0$	$K_{t_\phi} = 1$
$H_{e_y}(s) = K_{e_y} (T_{e_y}s + 1) e^{-\tau_{e_y}}$	$K_{e_y} = 0.15, T_{e_y} = 1 \text{ s}, \tau_{e_y} = 0.1 \text{ s}$			
$H_{e_\phi}(s) = K_{e_\phi} e^{-\tau_{e_\phi}}$	$K_{e_\phi} = 2.5, \tau_{e_\phi} = 0.25 \text{ s}$			
$H_y(s) = 0, H_\phi(s) = 0$				

IDENTIFICATION

This section addresses the second objective, that is to identify from experimental data whether the human pilot indeed employs feedforward control techniques, as hypothesized. For identification we wish to use a black box model for which no assumptions concerning the underlying dynamics of the system have to be made. More specifically, the system identification method of choice is one based on Linear Time Invariant ARX models, because such models have been used successfully for pilot control dynamics identification before (Ref. 20).

Identification approach

Ideally, we would like to find a method to identify transfer functions H_{t_y} and H_{t_ϕ} directly from experimental data. In order to do so, the signal ϕ_t (see Figs. 4 and 5) would have to be measurable. However, since ϕ_t is a signal that only “exists” in the human, this is not possible. The derivation to be presented next will show it is, however, possible to collect indirect evidence for the existence of feedforward action in the human pilot. In order to do so, one will have to make two assumptions on the form of H_{e_y} and H_{e_ϕ} .

First, we derive the lumped transfer function from f_t and e_y to u , based on Fig. 3. We can write u as a function of all the basic inputs to the ‘human controller box’:

$$u = (H_{t_\phi} \phi_t + H_{e_\phi} e_\phi + H_\phi \phi) H_{nms} \quad (10)$$

with

$$\phi_t = H_{t_y} f_t + H_{e_y} e_y + H_y y \quad (11)$$

We further note that:

$$e_\phi = \phi_t - \phi \quad (12)$$

and that

$$e_y = f_t - y \rightarrow y = f_t - e_y \quad (13)$$

Substituting Eq. 11, 12 and 13 into Eq. 10, we find the following equation:

$$\begin{aligned} u = & H_{nms} (H_{t_\phi} + H_{e_\phi}) (H_{t_y} + H_y) f_t \\ & + H_{nms} (H_{t_\phi} + H_{e_\phi}) (H_{e_y} - H_y) e_y \\ & + H_{nms} (H_\phi - H_{e_\phi}) \phi \end{aligned} \quad (14)$$

We further note that the following relations exist:

$$y = \phi C_y \rightarrow \phi = y C_y^{-1} \quad (15)$$

Substituting Eqs. 15 and 13 into Eq. 14 results in the following equation:

$$\begin{aligned} u = & H_{nms} \left((H_{t_\phi} + H_{e_\phi}) (H_{t_y} + H_y) + (H_\phi - H_{e_\phi}) C_y^{-1} \right) f_t \\ & + H_{nms} \left((H_{t_\phi} + H_{e_\phi}) (H_{e_y} - H_y) - (H_\phi - H_{e_\phi}) C_y^{-1} \right) e_y \end{aligned} \quad (16)$$

When using an LTI ARX model using input signals f_t and e_y and output signal u one will obtain the following two ‘lumped’ transfer function estimates:

$$\begin{aligned} Y_{f_t} &= \left((H_{t_\phi} + H_{e_\phi}) (H_{t_y} + H_y) + (H_\phi - H_{e_\phi}) C_y^{-1} \right) H_{nms} \\ Y_{e_y} &= \left((H_{t_\phi} + H_{e_\phi}) (H_{e_y} - H_y) - (H_\phi - H_{e_\phi}) C_y^{-1} \right) H_{nms} \end{aligned} \quad (17)$$

That is, the ARX method estimates the parameters of the ARX model given in Eq. 18 in a least-squares fashion, from which the estimates $Y_{f_t} = B_{f_t}(q)/A(q)$ and $Y_{e_y} = B_{e_y}(q)/A(q)$ are obtained.

$$A(q)u(t) = B_{f_t}(q)f_t(t) + B_{e_y}(q)e_y(t) + \varepsilon(t) \quad (18)$$

In Eq. 18 the parameters $A(q)$ and $B(q)$ are polynomials of order n_a and n_b , respectively, and ε the modeling residual. Fig. 7 is a schematic representation of the ARX model.

From observing Eq. 17, one can see why it is not possible to directly obtain estimates for H_{t_y} and H_{t_ϕ} : there are seven unknowns (all transfer functions indicated with “H”) and only two equations. We therefore look for possibilities to isolate

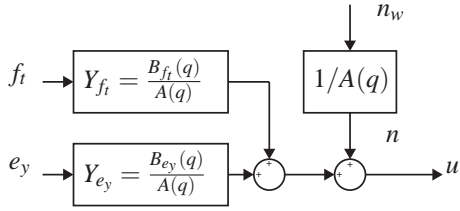


Fig. 7. Schematic representation of the ARX model with two input signals and one output signal and the two transfer functions the model will estimate.

H_{t_y} and H_{t_ϕ} as much as possible. Hence, we add estimates Y_{f_t} and Y_{e_y} together to find $Y_{f_t+e_y}$.

$$Y_{f_t+e_y} = Y_{f_t} + Y_{e_y} = (H_{t_\phi} + H_{e_\phi})(H_{t_y} + H_{e_y})H_{nms} \quad (19)$$

By adding Y_{f_t} and Y_{e_y} together, we eliminate the contribution of state feedback elements H_ϕ and H_y such that comparable control behavior in the pilot does not affect the analysis and it can not, by mistake, be identified as feedforward behavior. It is important to understand that $Y_{f_t+e_y}$ does not have a physical meaning, but that it does potentially allow us to find indirect evidence for feedforward behavior in H_{t_y} and H_{t_ϕ} , by making assumptions on the dynamics of H_{e_y} , H_{e_ϕ} and H_{nms} .

First, for the neuromuscular dynamics H_{nms} we assume the second-order model as given in Eq. 3. This model is based on experimental data and describes the inherent neuromuscular dynamics of the arm, which mainly influence pilot dynamics at frequencies above 7 rad/s. As this control task is similar to previous experiments, we assume these dynamics to be identical.

Then, we observe the form of transfer functions H_{t_y} , H_{t_ϕ} , H_{e_y} and H_{e_ϕ} from a control theoretical perspective. The roll error feedback element H_{e_ϕ} is most likely a gain, see Eq. 4, and the lateral error feedback element H_{e_y} is most likely a gain at lower frequencies and a single differentiator (or *lead*) at higher frequencies, see Eq. 8. The two feedforward elements H_{t_y} and H_{y_ϕ} are in the ideal case a double and a single differentiator, respectively. Hence, if one were to compare the $Y_{f_t+e_y}$ dynamics of a controller with and without feedforward and the aforementioned assumptions were true, distinct differences are to be seen.

The next section will elaborate on these differences and show, by means of simulation, that such differences can indeed be identified by means of LTI models.

Verification using simulations

The result of Eq. 19 is to be verified by means of simulations, for each of the four different parameter sets of the pilot model developed in the preceding sections of the paper, see Table 1. From the simulated signals f_t , e_y , and u we estimate Y_{f_t} and Y_{e_y} by means of an ARX model, from which $Y_{f_t+e_y}$ can be calculated.

Simulations with and without human remnant are performed. Human remnant is defined by Ref. 6 as all nonlinearities in the human and all control inputs uncorrelated to

the pilot input signals. We observe the results for simulations free of human remnant first.

Fig. 8 (next page) shows a Bode plot of the theoretical dynamics of $Y_{f_t+e_y}$ and those estimated from the simulated signals, for all four settings of the model. At frequencies lower than approximately 7 rad/s, the dynamics of H_{t_y} , H_{t_ϕ} , H_{e_y} , and H_{e_ϕ} determine the dynamics of $Y_{f_t+e_y}$. At higher frequencies, a peak in the magnitude is seen due to the neuromuscular dynamics, H_{nms} . Two important observations can be made concerning the dynamics at frequencies lower than 7 rad/s.

First, one can see that the $Y_{f_t+e_y}$ transfer function is markedly different for the four different model settings. For the FB model $Y_{f_t+e_y}$ is a single differentiator above 0.7 rad/s. The corresponding phase is determined largely by the lead term in H_{e_y} and the time delay in H_{e_ϕ} . The phase rises slightly above 0 deg around 2 rad/s, but then rapidly falls off due to the time delay.

On the other hand, the $Y_{f_t+e_y}$ transfer function of the models that contain one or two feedforward paths have a much steeper magnitude slope, and more phase lead compared to the FB model. The effect of lateral feedforward is clear for frequencies above 1 rad/s, both in magnitude and in phase, as can be seen from comparing the LFF model to the FB model and the RLFF model to the RFF model. The effect of roll feedforward (compare RFF to FB) is less clear, and only affects the magnitude and phase above 5 rad/s. The effect of the two feedforward paths on the $Y_{f_t+e_y}$ transfer function compared to the FB model is a steeper magnitude slope and a more positive phase. It is important to note that the absolute magnitude and phase values depend on the chosen model parameter values, but that the differences between the different models remain the same.

The second observation to be made from Fig. 8 is that the estimates of the $Y_{f_t+e_y}$ transfer function estimated from simulated data with our proposed identification method are almost identical to the corresponding theoretical solutions. This shows that the ARX method is very successful in estimating the underlying dynamics for a noise free simulation and also serves as a check on the derivations made earlier in this section.

Obviously, the data to be measured in a human-in-the-loop experiment will contain human remnant and therefore simulations including simulated human remnant were also performed. The simulated remnant is obtained by filtering a white noise signal with a third-order low-pass filter and adding this signal to the control signal u during the simulation. The white noise filter is defined as in Eq. 20, with $\omega_n = 12.7$ rad/s and $\zeta_n = 0.26$, based on Ref. 17.

$$H_n(s) = \frac{K_n \omega_n^3}{(s^2 + 2\zeta_n \omega_n s + \omega_n^2)(s + \omega_n)} \quad (20)$$

The gain K_n was set to 0.2, such that the variance of the remnant signal was approximately 15% of the variance of the total control signal u .

Fig. 9 shows the estimated $Y_{f_t+e_y}$ transfer function of 20 individual simulations with simulated remnant for each of the

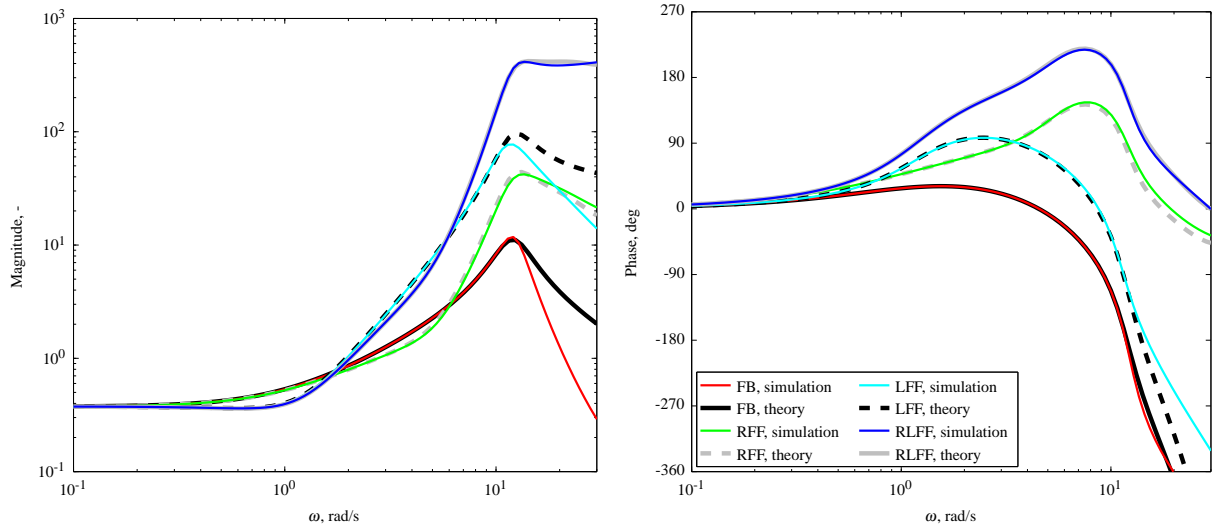


Fig. 8. Simulated estimation of $Y_{f_i+e_y}$ compared to the analytical solution, for four different parameter sets of the feedforward gains K_{t_y} and K_{t_ϕ} . Without simulated remnant.

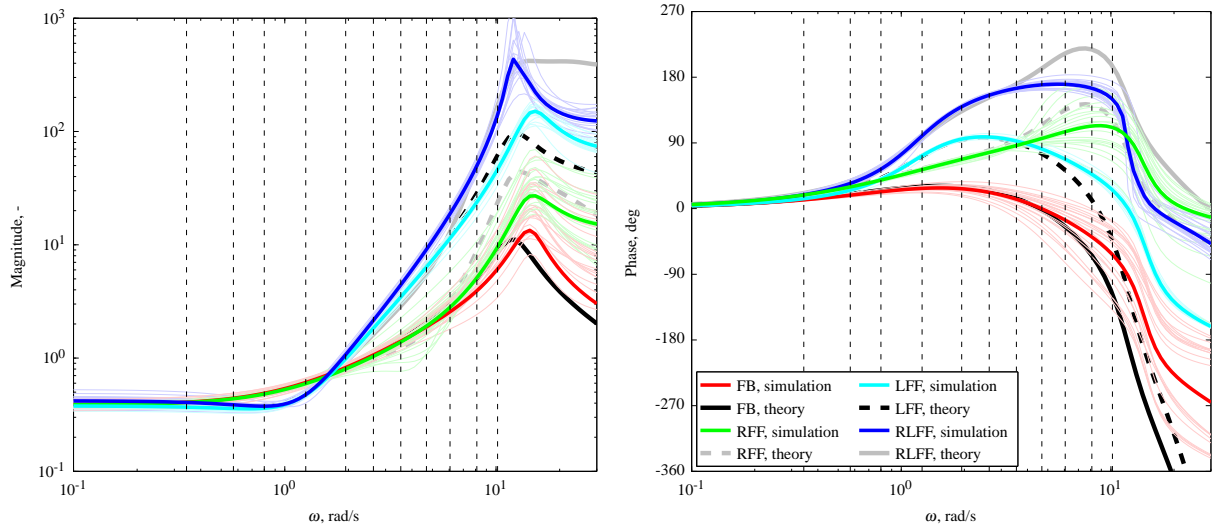


Fig. 9. Simulated estimation of $Y_{f_i+e_y}$ compared to the analytical solution, for different settings of the feedforward gains K_{t_y} and K_{t_ϕ} . With simulated remnant.

four model settings with a thin, light colored line and the average of those 20 simulations with a thick, darker colored line. The figure shows that the estimated frequency responses of $Y_{f_i+e_y}$ are not exactly identical to the theoretical solutions due to the remnant, especially at higher frequencies. The important features of the $Y_{f_i+e_y}$ dynamics, that enables one to distinguish one parameter set from the other are, however, still clearly visible. That is, the models that contain either roll, lateral or both feedforward paths still have a much steeper magnitude curve at frequencies above 1 rad/s and a clearly positive phase until 10 rad/s. Hence, we conclude that despite human remnant it is possible to distinguish purely feedback control behavior from behavior that also involves feedforward control

strategies.

EXPERIMENT

Method

To collect measurements of human pilots performing a lateral reposition task, a human-in-the-loop experiment was conducted.

Apparatus The experiment was performed on the MPI CyberMotion Simulator (CMS) at the Max Planck Institute for Biological Cybernetics (Ref. 21). The CMS is a motion simulator based on an anthropomorphic robot manufactured by

KUKA Roboter GmbH. Recently, two major developments on the CMS were completed such that the current design differs significantly from that described in Ref. 21. First, a completely enclosed cabin to be used as subject station was developed containing a wide field-of-view visualization system. Secondly, the entire anthropomorphic robot was placed on a 9.6 m long linear axis, allowing for a very large lateral or longitudinal motion space (depending on the robot orientation), see Fig. 10.

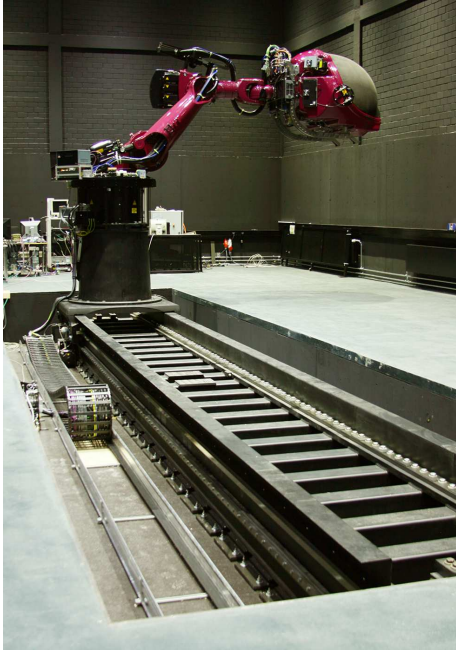


Fig. 10. The MPI CyberMotion Simulator on a linear axis and with the enclosed pilot station at the end of the anthropomorphic robot arm.

The roll motion was presented as pure roll motion (no washout) with a motion gain of 0.5 using the rotational joint closest to the pilot cabin (Ref. 21). The lateral motion was presented as pure lateral motion (no washout) with a motion gain of 0.06 using the linear axis, to scale down the large lateral motion (400 ft or 121.9 m) of the lateral reposition to the available lateral motion space of 9.6 m.

Subjects used the left/right axis of an electrical control loaded helicopter cyclic stick (Wittenstein Aerocontroller) to give control inputs. Subjects experienced a stiffness of 32 N rad⁻¹, a damping force of 2.14 N s rad⁻¹ and a mass of 0.4 N s² rad⁻¹, at the hand contact point located 35 cm above the point of rotation. The maximum lateral stick deflection was ± 17 deg, the longitudinal axis of the stick was locked. The stick gain was set to 3, such that u equaled three times the stick deflection in radians.

The visuals were generated by the game development system Unity (Ref. 22) version 4.0.0f7 and represented the ADS-33 lateral reposition setting as provided in Ref. 12, see Fig. 11. A clearly visible white circle appeared in the 3D world indicating the current position of the target f_t . Another, smaller, but also clearly visible red circle appeared in the 3D world



Fig. 11. Experiment visuals.

indicating the current lateral position of the helicopter y . It was the objective of the subjects to control the helicopter such that the distance between the two circles was minimized at all times. Time delay measurements of the visual system were performed throughout the experiment and were approximately 40 ms.

Forcing functions The lateral target signal f_t was as shown in Fig. 1. The onset of each lateral reposition was made clear to the subjects by means of a timer counting down from 5 to 0 seconds. The countdown text was only visible while counting down and was placed such that it did not impair the subjects ability to maintain a stable hover, but was still clearly visible.

The roll disturbance signal $f_{d\phi}$ was a sum-of-sinusoid signal, appearing random to the human and consisted of eleven sinusoids, as defined in Eq. 21 (in radians).

$$f_{d\phi}(t) = K_{d\phi} \sum_{k=1}^{11} A_{\phi_k} \sin\left(\frac{2\pi}{T_m} n_{\phi_k} t + \varphi_{\phi_k}\right) \quad (21)$$

In Eq. 21, T_m designates the measurement time and is equal to 55 s. Parameters A_{ϕ_k} , n_{ϕ_k} and φ_{ϕ_k} are defined in Table 2. Gain $K_{d\phi}$ scaled the magnitude of the disturbance signal and was set to 4 to obtain a disturbance signal with a standard deviation of 4 deg. The Power Spectral Density of both the lateral target

Table 2. Roll disturbance signal $f_{d\phi}$ sinusoid properties.

k	n_{ϕ_k}	A_{ϕ_k}	φ_{ϕ_k}	k	n_{ϕ_k}	A_{ϕ_k}	φ_{ϕ_k}
1	3	0.7	3.0164	7	31	0.07	3.0773
2	5	0.7	3.6567	8	41	0.07	2.7997
3	7	0.7	1.6974	9	53	0.07	4.0609
4	11	0.7	4.8099	10	71	0.07	4.4571
5	17	0.07	4.9964	11	87	0.07	4.7418
6	23	0.07	1.1742				

signal f_t and the roll disturbance signal $f_{d\phi}$ is given in Fig. 12, as well as a time history.

Procedure and independent measures Subjects performed the lateral reposition task until they reached a plateau in their performance. Then, 10 measurement runs were recorded for which all analyses are performed. Task performance was measured by the root-mean-square of e_y and was reported to the subjects after each trial to motivate subjects to perform as

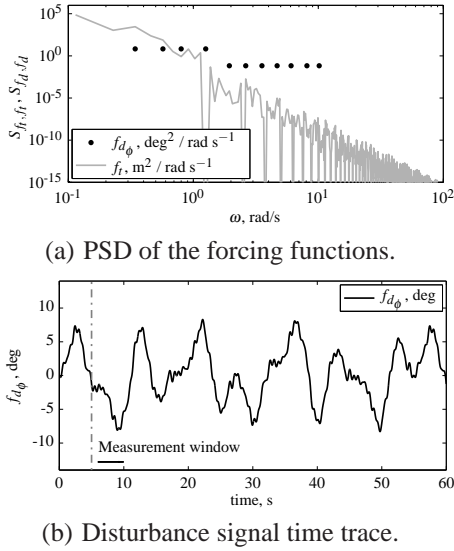


Fig. 12. The power spectral density and time histories of the roll disturbance signal $f_{d\phi}$.

good as possible. The individual tracking runs lasted 60 seconds, of which the last 55 seconds were used as the measurement data. The time traces of all system outputs, ϕ and y , the tracking error e_y , and the control signal u were recorded.

Subjects Four subjects participated in the experiment, all males, with an average age of 32 years. One of the subjects was a retired helicopter pilot with approximately 110 flight hours. The other three subjects obtained familiarity with helicopter dynamics through radio controlled model helicopters and fixed-base helicopter simulators.

Dependent measures

Performance measures Both the root-mean-square of the lateral tracking error, $\text{RMS}(e_y)$, and the maximum lateral tracking error, $\max(e_y)$, are calculated from the measured time traces.

Control behavior identification By means of a Linear Time Invariant ARX model, the frequency responses Y_{f_i} and Y_{e_y} are identified for each of the ten measured runs of each subject separately. From these estimates the sum $Y_{f_i+e_y} = Y_{f_i} + Y_{e_y}$ is calculated. The ten obtained frequency responses are averaged and compared to $Y_{f_i+e_y}$ frequency responses obtained from the model developed in this paper.

The amount of free parameters of the ARX identification method will be chosen such that it is able to capture the relevant dynamics hidden in all the measured data, without overfitting. More precisely, the amount of free parameters is increased while observing the stability of the estimated ARX models and the quality of the fit, for each run of each subject. The quality of the ARX model fit on each run is measured by the Variance Accounted For, defined as:

$$\text{VAF} = \left(1 - \frac{\sum_{k=0}^N |u(k) - \hat{u}(k)|^2}{\sum_{k=0}^N u(k)^2} \right) \times 100\% \quad (22)$$

In Eq. 22, \hat{u} is the modeled and u is the measured control signal. As soon as adding one parameter causes one of the 40 ARX models to become unstable or the average VAF decreases, calculated over all 40 runs, no more free parameters are added.

Hypotheses

Given the resulting task performance benefit compared to pure feedback control, we hypothesize that for the lateral reposition task considered in this paper pilots will utilize feedforward control. Furthermore, we expect that our proposed ARX identification method will show that evidence of feedforward behavior can be identified from experimental data.

RESULTS

Performance measures

Fig. 13 shows the performance of the participants as they performed the experiment runs. Fig. 13(a) shows the RMS value of the lateral position error, e_y , calculated over the entire measurement window of 55 seconds for each run. Fig. 13(b) shows the maximum lateral position error at any time within the measurement window.

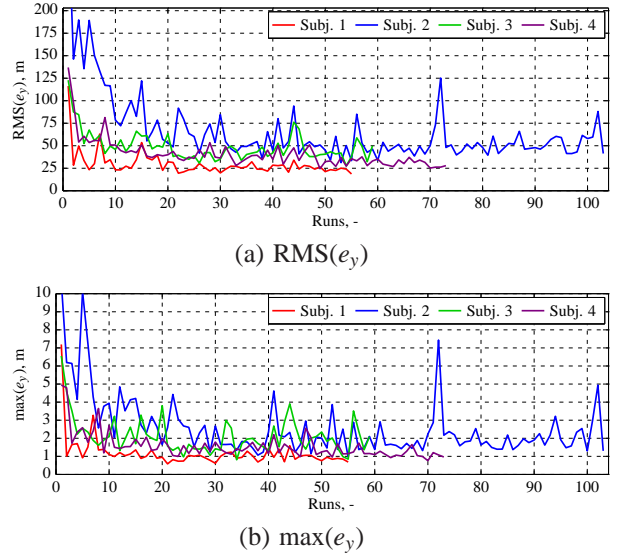


Fig. 13. Performance scores $\max(e_y)$ and $\text{RMS}(e_y)$ for all runs performed by all four subjects. The last 10 runs of each subject are the measurement runs.

Both figures show that all participants reached a plateau in their performance after 20 to 30 runs and that there is a clear correspondence between both the performance metrics. Performing up to 80 additional runs (participant 2) did not allow participants to further improve their performance. The figures also show that all participants showed significant spread in their error scores between runs. Differences between subsequent runs are sometimes as large as 50 to 100%. This shows that the task at hand was a difficult task and was sensitive for

small control errors that quickly led to large lateral tracking errors.

Comparing the experimental results of Fig. 13(b) with the simulation results of Fig. 6 for $K_{d\phi} = 4$ deg, we note that the best human performance ($\max(e_y) = 0.58$ m for subject 1; 0.95 m for subject 2; 0.81 m for subject 3; 0.76 m for subject 4) is better than the performance of the purely feedback model, the FB model, ($\max(e_y) = 3.0$ m) and worse than the RLFF model containing both feedforward paths ($\max(e_y) = 0.28$ m).

Time histories

Fig. 14 shows the lateral error signals e_y of the ten measurement runs of each subject and the mean of those runs. One

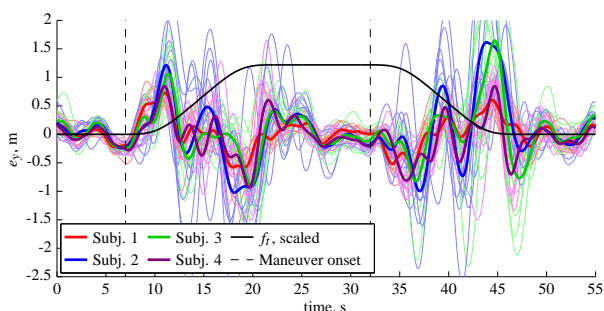


Fig. 14. Theory tested with data from the test experiment.

can see that all subjects consistently lagged behind the target during the first 5 seconds after the onset of each maneuver (marked in the figure), despite being informed by the count-down exactly when the target would start moving. Subjects also consistently overshoot the end position of the lateral reposition, although it was very clear from the visual scene where the target would stop moving.

Identification

Free ARX model parameters The amount of free parameters of the ARX model was increased until the average quality of fit, measured by the Variance Accounted For and calculated over all ten runs of all four subjects, decreased due to overfitting. Fig. 15 shows the VAF of each of the ten measurement runs of all four subjects and the average for an increasing amount of free parameters. The figure shows that the maximum average quality of fit was found for $n_a = 4$ and $n_b = 3$. All results presented in the remainder of this section were calculated for $n_a = 4$ and $n_b = 3$.

ARX model fit quality ARX models were fit to the ten measurement runs of each subject to identify the control dynamics of the human pilots, which resulted in estimates of Y_{f_t} and Y_{e_y} . The obtained models were all stable, such that the Variance Accounted For could be calculated by Eq. 22 for each measurement run, see Fig. 16. The mean VAF of the ARX fits was between 70 and 80%, which shows that the model was successful in capturing the pilot control dynamics and suggests

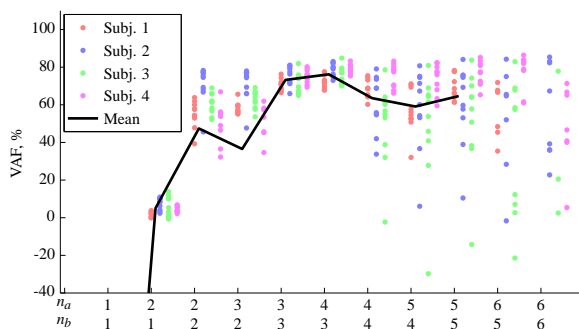


Fig. 15. The average VAF of all ten measurement runs for all subjects and the mean over all runs, as a function of the amount of free parameters.

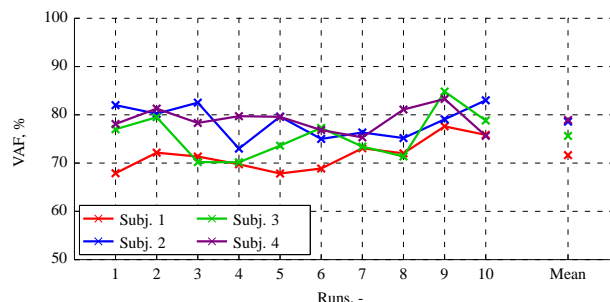


Fig. 16. VAF of the ten measurement runs for all subjects and the mean over all runs for $n_a = 4$ and $n_b = 3$.

that the estimates of Y_{f_t} and Y_{e_y} are a good characterization of the pilot behavior.

ARX model fits The transfer functions Y_{f_t} and Y_{e_y} identified by means of the ARX method were added together to obtain $Y_{f_t+e_y}$ as defined in Eq. 19. Fig. 17 presents the frequency response functions of $Y_{f_t+e_y}$ of all ten measurement runs and the average over all ten runs, for each subject. The figure shows that $Y_{f_t+e_y}$ is consistent throughout all the runs for each subject. This suggests that the behavior of the subjects was constant and that the mean is a good representation of the data.

Fig. 18 shows only the $Y_{f_t+e_y}$ frequency response averaged over the ten measurement runs, to reduce clutter and improve clarity. Two important observations can be made from the figure.

First, the estimated dynamics are reasonably consistent across subjects, although differences exist. The magnitude of $Y_{f_t+e_y}$ appears to be a gain at low frequencies for all but one subject. Around 0.5 rad/s the slope of the magnitude curves increase and becomes steeper than a single differentiator, but not quite as steep as a double differentiator. At approximately 6 rad/s the slope of the magnitude curve reduces and above those frequencies the neuromuscular peak can be observed. For most subjects this peak is located at a slightly lower frequency (around 7 rad/s) than normally seen in tracking tasks (around 12 rad/s).

The phase of $Y_{f_t+e_y}$ is close to zero at lower frequencies and gradually increases to more positive values. Around 3

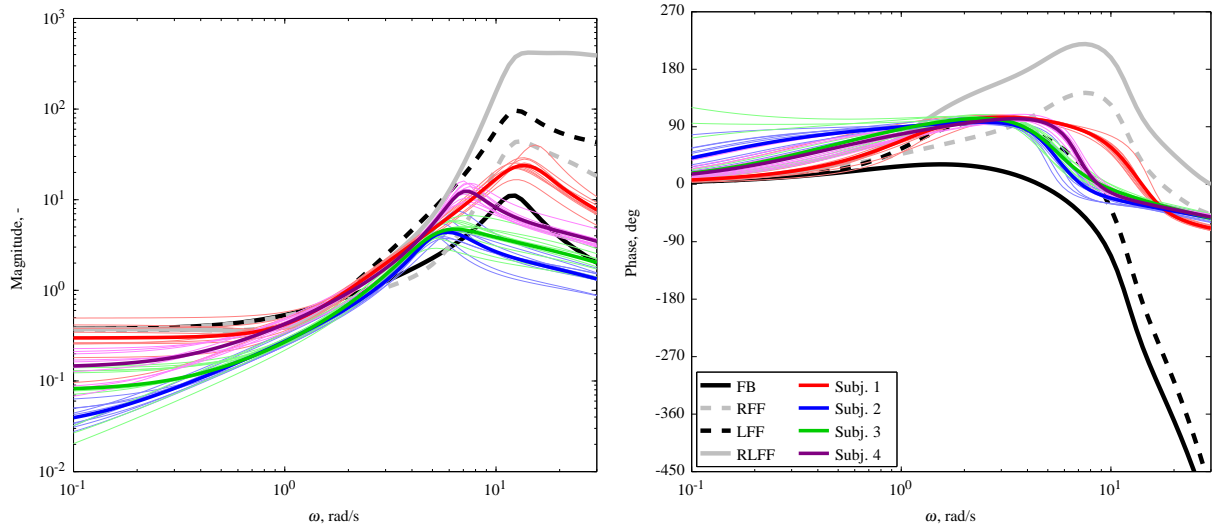


Fig. 17. Estimate of $Y_{f_t+e_y}$ identified from single tracking runs and the average per subject.

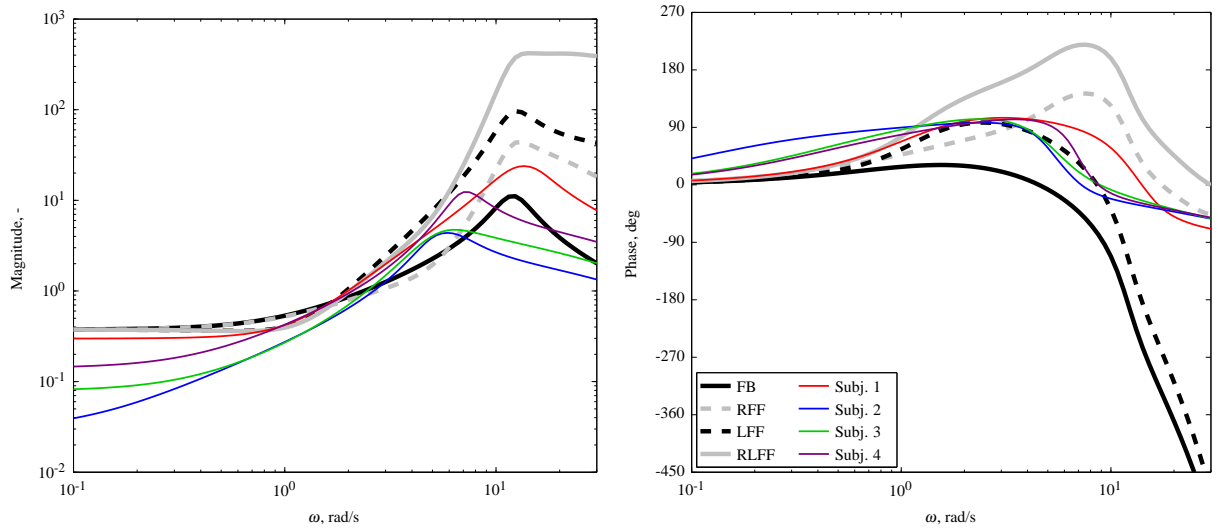


Fig. 18. The per subject average of the estimated $Y_{f_t+e_y}$ and theoretical $Y_{f_t+e_y}$ response functions based on the model developed in this paper.

rad/s the phase peaks slightly above 90 degrees and then drops off to lower values. The phase curve is very consistent across subjects.

The second important observation is that the $Y_{f_t+e_y}$ curves of the subjects seem to contain some key characteristics that are also seen in the $Y_{f_t+e_y}$ curves for the feedforward models. That is, the magnitude slope is steeper than a single differentiator and the phase is clearly well above zero, which is an indication for feedforward behavior. However, the experimentally measured curves are certainly not a perfect fit to any of the feedforward model curves, which calls for further research.

DISCUSSION

In this paper, a helicopter pilot model for a tracking task representative of the ADS-33 lateral reposition maneuver was developed. The model consists of both a feedback loop and two feedforward paths, containing the inverse of the helicopter roll and lateral system dynamics. This model and the results of a pilot-in-the-loop experiment were used to investigate the two main objectives of this paper, being 1) to investigate by means of simulation how the performance of the pilot-helicopter system depends on the presence of feedforward behavior and 2) to identify from experimental data whether or not the human pilot indeed employs such feedforward control techniques.

By means of simulations we showed that the tracking performance depends strongly on the inclusion of the feedfor-

ward paths in a realistic control task. That is, the performance of the model including both roll and lateral feedforward is one order of magnitude better than the purely feedback model. Although the absolute performance of the model depends on the chosen numerical values of the model parameters, it is interesting to note that the best performance of all subjects in the experiment was clearly better than the modeled pure feedback performance. Obviously, a comparison based on a single performance metric is not conclusive for the underlying pilot behavior, but it does support our motivation to investigate feedforward behavior in the human pilot. That is, if a simulated pilot model is used early in the design process to predict the performance level of the helicopter it is important that the model does not grossly over or underestimate the performance.

Our second objective was to identify the hypothesized feedforward control behavior during a human-in-the-loop experiment. We found that it is impossible to directly identify the hypothesized feedforward behavior. Because the pilot is able to control on a large amount of input signals seven different control responses are to be identified; two of them are feedforward elements. Direct identification would require one to measure the commanded roll signal, ϕ_t , which is a signal ‘internal’ to the pilot and can therefore not be measured.

Ref. 5 solved this problem by additionally presenting a roll target signal that corresponded to the presented lateral target signal f_t and assuming this additional signal to be identical to the internal roll command. This assumption, however, only holds in cases where there are no disturbances on the roll motion and the pilot makes no control errors. As soon as disturbances or errors are introduced, the pilot will have to decide between tracking the roll angle needed to correct for lateral errors and tracking the explicitly presented roll target.

In this paper we took a different approach and made use of the fact that the error feedback and feedforward dynamics can be estimated in a ‘lumped’ form, designated $Y_{f_t+e_y}$, reducing the amount of unknown control elements to five, being the roll and lateral feedforward elements and the neuromuscular system dynamics. Then, by making assumptions on the content of three of those control elements based on control theory, human physiology and previous experiments, evidence for feedforward behavior can be collected. More precisely, the dynamics of the term $Y_{f_t+e_y}$ would contain at most one differentiator and have a zero or negative phase in case of predominantly feedback behavior. Estimated dynamics of $Y_{f_t+e_y}$ containing a steeper magnitude slope than one differentiator and a mostly positive phase response would point in the direction of feedforward control behavior. Tests by means of model simulations confirmed this approach to be feasible, after which a human-in-the-loop experiment was performed.

The $Y_{f_t+e_y}$ dynamics measured from human subjects contain characteristics similar to the $Y_{f_t+e_y}$ curves obtained from the pilot model containing feedforward, although not as clearly as one might expect. That is, the measured curves are certainly not a perfect fit to the feedforward model, but

do achieve a higher magnitude slope than a single differentiator and have a clearly more positive phase response than the purely feedback model. This suggests that our proposed transfer functions for the feedforward terms are not perfect. We see this as an additional motivation for further research into helicopter pilot modeling by means of physiologically valid pilot models and human-in-the-loop experiments.

To put this study into the proper perspective, it is important to note that several modifications of the original ADS-33 lateral reposition task had to be made in order to measure the pilot control dynamics. The most radical modification is that the task was changed from a ‘free’ control task into a tracking task, exactly prescribing the lateral position of the helicopter throughout the entire maneuver. The ADS-33 specifies the lateral reposition task by prescribing the amount of distance that needs to be covered by lateral motion within a certain time. Theoretically, the maneuver can be flown in many different ways, but taking into account the stringent longitudinal, vertical and heading motion requirements the amount of ‘acceptable’ maneuver trajectories is strongly reduced. That is, in practice the pilot will attempt to keep the helicopter within a narrow range of an *imaginary* reference trajectory for which all requirements are met at the same time. Therefore, the tracking task is probably similar, but not exactly the same as the original task and small differences in control behavior may still be expected.

Additionally, the dynamics of the helicopter were simplified to simple linear transfer functions neglecting, amongst others, coupling and drag effects. Especially the roll dynamics were simplified considerably to make the task easier. The roll dynamics were a single integrator, where more realistic transfer function models also consider the unstable lateral phugoid, lateral sway damping and roll damping (Ref. 23). The more complex dynamics would require the pilot to also generate lead at higher frequencies in the roll loop and continuously stabilize the unstable lateral phugoid, which would not only make the task more difficult but would also affect the identification problem.

Based on the presented results and our experience with this experiment we provide the following recommendations for future research.

First, it is important to better understand the assumptions concerning the error feedback elements that need to be made to obtain evidence of feedforward behavior and to validate them by means of human-in-the-loop experiments. This validation should preferably be done simultaneously to the feedforward identification, because due to the adaptive nature of the human it is difficult to assume certain control dynamics to remain constant across different control tasks and experiments.

Furthermore, our current approach was to qualitatively compare the overall ‘shape’ of the measured $Y_{f_t+e_y}$ dynamics to the shape of the $Y_{f_t+e_y}$ dynamics of the models. It would be more objective to define a metric by which these dynamics can be compared quantitatively and to investigate which model parameters affect the similarity in particular.

Finally, it is important to investigate how the way the task is defined and presented to the pilots affect their behavior. In this study the task was presented as a tracking task in order to make use of validated system identification methods, but this does not exactly represent the ADS-33 certification task.

CONCLUSIONS

This paper investigated helicopter pilot control behavior in a tracking task resembling an ADS-33 lateral reposition task. Based on control theoretical concepts and knowledge of human physiology and perception, we hypothesized that the inclusion of an inverse system dynamics feedforward path is necessary to obtain an accurate prediction of helicopter performance. From simulations we conclude that the performance of the pilot-helicopter system is one order of magnitude better for a pilot model that includes feedforward action than for a pure feedback pilot model. It was found that the feedforward control dynamics can not be identified from experimental data directly, but that indirect evidence *can* be collected for the existence of feedforward action, by making reasonable assumptions on the feedback control behavior. Results from a human-in-the-loop experiment in which four subjects performed the lateral reposition task suggest evidence for the conclusion that the human pilot utilizes feedforward strategies, but does not result in a complete pilot model for this task.

ACKNOWLEDGMENTS

H. H. Bülthoff was supported by the World Class University program through the National Research Foundation of Korea funded by the Ministry of Education, Science and Technology (R31-10008), and by the myCopter project, funded by the European Commission under the 7th Framework Program.

REFERENCES

- ¹Hess, R. A., "Simplified Technique for Modeling Piloted Rotorcraft Operations Near Ships," *Journal of Guidance, Control, and Dynamics*, Vol. 29, (6), 2006, pp. 1339–1349.
- ²Lee, D., Sezer-Uzol, N., Horn, J. F., and Long, L. N., "Simulation of Helicopter Shipboard Launch and Recovery with Time-Accurate Airwakes," *Journal of Aircraft*, Vol. 42, (2), 2005, pp. 448–461.
- ³Celi, R., "Analytical Simulation of ASDS-33 Mission Task Elements," Proc. of the AHS 63rd Annual Forum, May 2007.
- ⁴Bottasso, C. L., Maisano, G., and Scorcelletti, F., "Trajectory Optimization Procedures for Rotorcraft Vehicles Including Pilot Models, with Applications to ADS-33 MTEs, Cat-A and Engine Off Landings," Proc. of the AHS 65th Annual Forum, May 2009.
- ⁵Nieuwenhuizen, F. M., Zaal, P. M. T., Teufel, H. J., Mulder, M., and Bülthoff, H. H., "The Effect of Simulator Motion on Pilot Control Behaviour for Agile and Inert Helicopter Dynamics," Proc. of the 35th European Rotorcraft Forum, Hamburg, Germany, September 22–25 2009.

⁶McRuer, D. T. and Jex, H. R., "A Review of Quasi-Linear Pilot Models," *IEEE Trans. on Human Factors in Electronics*, Vol. HFE-8, (3), 1967, pp. 231–249.

⁷Hess, R. A., "Structural Model of the Adaptive Human Pilot," *Journal of Guidance, Control, and Dynamics*, Vol. 3, (5), 1980, pp. 416–423.

⁸Kleinman, D. L., Baron, S., and Levison, W. H., "An optimal control model of human response part I: Theory and validation," *Automatica*, Vol. 6, (3), May 1970, pp. 357–369.

⁹Whalley, M. S., "Development and Evaluation of an Inverse Solution Technique for Studying Helicopter Maneuverability and Agility," NASA Technical Memorandum 102889, NASA Ames Research Center, Moffett Field (CA), July 1991.

¹⁰Thomson, D. and Bradley, R., "Inverse simulation as a tool for flight dynamics research - Principles and applications," *Progress in Aerospace Sciences*, Vol. 42, 2006, pp. 174–210.

¹¹Cameron, N., Thomson, D. G., and Murray-Smith, D. J., "Pilot modelling and inverse simulation for initial handling qualities assessment," *The Aeronautical Journal*, Vol. 107, (1074), 2003, pp. 511–520.

¹²Anon., "Aeronautical Design Standard ADS-33-E. Handling qualities requirements for military rotorcraft." Technical report, United States Army Aviation and Missile Command, Aviation Engineering Directorate, Redstone Arsenal, Alabama, March 2000.

¹³Gottsdanker, R. M., "The Ability of Human Operators to Detect Acceleration of Target Motion," *Psychological Bulletin*, Vol. 53, (6), 1956, pp. 477–487.

¹⁴Gum, D. R., "Modeling of the Human Force and Motion-Sensing Mechanisms," Technical Report AFHRL-TR-72-54, Air Force Human Resources Laboratory, Wright-Patterson Air Force Base (OH), June 1973.

¹⁵Zaal, P. M. T., Pool, D. M., De Bruin, J., Mulder, M., and Van Paassen, M. M., "Use of Pitch and Heave Motion Cues in a Pitch Control Task," *Journal of Guidance, Control, and Dynamics*, Vol. 32, (2), March–April 2009, pp. 366–377.

¹⁶Krendel, E. S. and McRuer, D. T., "A Servomechanics Approach to Skill Development," *Journal of the Franklin Institute*, Vol. 269, (1), 1960, pp. 24–42.

¹⁷Zaal, P. M. T., Pool, D. M., Chu, Q. P., Van Paassen, M. M., Mulder, M., and Mulder, J. A., "Modeling Human Multimodal Perception and Control Using Genetic Maximum Likelihood Estimation," *Journal of Guidance, Control, and Dynamics*, Vol. 32, (4), 2009, pp. 1089–1099.

¹⁸Drop, F. M., Pool, D. M., Damveld, H. J., van Paassen, M. M., and Mulder, M., "Identification of the Feedforward Component in Manual Control With Predictable Target Signals," *Cybernetics, IEEE Transactions on*, Vol. PP, (99), 2013, pp. 1–14.

¹⁹Wasicko, R. J., McRuer, D. T., and Magdaleno, R. E., "Human Pilot Dynamic Response in Single-loop Systems with Compensatory and Pursuit Displays," Technical Report AFFDL-TR-66-137, Air Force Flight Dynamics Laboratory, December 1966.

²⁰Nieuwenhuizen, F. M., Zaal, P. M. T., Mulder, M., Van Paassen, M. M., and Mulder, J. A., "Modeling Human Multichannel Perception and Control Using Linear Time-Invariant Models," *Journal of Guidance, Control, and Dynamics*, Vol. 31, (4), 2008, pp. 999–1013.

²¹Teufel, H. J., Nusseck, H.-G., Beykirch, K. A., Bulter, J. S., Kerger, M., and Bülthoff, H. H., "MPI Motion Simulator: Development and Analysis of a Novel Motion Simulator," Paper AIAA-2007-6476, Proc. of the AIAA Modeling and Simulation Technologies Conference, Hilton Head (SC), 20–23 August 2007.

²²Unity Technologies, "Unity 3D," <http://unity3d.com/>, 2013.

²³Heffley, R. K., "A Compilation and Analysis of Helicopter Handling Qualities Data, Volume Two: Data Analysis," Technical Report NASA Contract NAS2-9344, NASA, August 1979.